ELSEVIER

Journal of Magnetism and Magnetic Materials 200 (1999) 598–615

Journal of magnetism and magnetic materials

www.elsevier.com/locate/jmmm

Mössbauer-effect studies of multilayers and interfaces

T. Shinjo[a], W. Keune[b,*]

[a]*Institute for Chemical Research, Kyoto University, Uji, Kyoto-fu 611-0011, Japan*
[b]*Laboratorium für Angewandte Physik, Gerhard-Mercator-Universität Duisburg, D-47048 Duisburg, Germany*

Received 8 January 1999; received in revised form 10 March 1999; accepted 10 March 1999

Abstract

The usefulness of Mössbauer spectroscopy for the investigation of magnetic multilayer systems is described. By applying ^{57}Fe Mössbauer spectroscopy, the behavior of ultrathin magnetic layers, such as FCC-like Fe films on Cu(0 0 1), is studied. Position-specified (depth-selective) information is available by preparing samples in which monatomic ^{57}Fe probe layers are placed at specific vertical positions, e.g. at interfaces or at the surface. As demonstrated for epitaxial chemically ordered $Fe_{50}Pt_{50}$ alloy films and polycrystalline nanostructured Tb/Fe multilayers, the Fe-spin structure can be determined directly, and a site-selective Fe-specific magnetic hysteresis loop can be traced in very-high-coercivity materials. For the studies of non-magnetic layers, on the other hand, hyperfine field observations by ^{197}Au and ^{119}Sn probes are worthwhile. Spin polarizations in Au layers penetrating from neighboring ferromagnetic 3D layers are estimated from ^{197}Au Mössbauer spectra and are also studied by inserted ^{119}Sn probes in Au/3D multilayers. In the Sn spectra for Cr/Sn multilayers, it was found that remarkably large spin polarization is penetrating into Sn layers from a contacting Cr layer, which suggests that Cr atoms in the surface layer have a ferromagnetic alignment.

Keywords: Mössbauer spectroscopy; Hyperfine fields; Spin polarization; Interface magnetism; Multilayer magnetism

1. Introduction

Mössbauer spectroscopy is a useful technique for the investigation of magnetism in ultrathin films, interfaces and multilayers. By observing magnetic hyperfine fields, B_{hf}, one is able to confirm the existence of magnetic order, and estimate the magnitude of the local moment and the direction of magnetization. The magnetic transition temperature is determined from the temperature dependence of the hyperfine field. The Mössbauer effect shows whether the thin-film or multilayer samples and their interfaces are composed of different metallurgical and magnetic phases. Information from Mössbauer spectroscopy is essentially element-specific and even position-selective if the Mössbauer-isotope probes are located as desired. For instance, by analyzing the spectra for topmost interface layers in a multilayer, we can provide structural information about the interface from a microscopic viewpoint [1].

Since the discovery of giant magnetoresistance (GMR) [2,3], novel problems have been raised up concerning magnetism of ultrathin films and interfaces. It is believed that the spin-dependent

* Corresponding author. Tel.: + 49-203-3792387; fax: + 49-203-3793601.

E-mail address: keune@uni-duisburg.de (W. Keune)

0304-8853/99/$ - see front matter
PII: S0304-8853(99)00346-7

scattering occurs mainly at interface sites, but the relation between interface roughness and the spin-dependent scattering probability is not yet clear. The mechanism of interlayer coupling between magnetic layers across a non-magnetic spacer layer is also a crucial issue, and the studies of magnetism in non-magnetic layers contacting with ferromagnetic layers are of great importance. For the studies of non-magnetic layers, ^{197}Au and ^{119}Sn are useful Mössbauer probes.

In this article, several studies using ^{57}Fe probes are briefly summarized, emphasizing the unique information which Mössbauer spectroscopy as a local atomistic technique may provide. Furthermore, studies of 3D/Au multilayers using ^{197}Au and ^{119}Sn probes are introduced. As the GMR effect has been observed for the first time in Fe/Cr multilayers, the role of the Cr spacer layer is also of interest. Finally, some preliminary Mössbauer results on ^{119}Sn in Cr/Sn systems are described.

2. Survey of ^{57}Fe Mössbauer studies

2.1. Interfaces

It is well known that ^{57}Fe is the most convenient isotope for Mössbauer measurements, and there are a large number of publications concerning Mössbauer spectroscopic studies of interface magnetism [1]. A recent review of structure and magnetism of some Fe mono- and multilayer systems as seen by conversion-electron Mössbauer spectroscopy (CEMS) at atomic scale was given by Przybylski [4]. If ^{57}Fe probes are located selectively at interfaces sites, the structure of the interface is conjectured from the hyperfine field observation. Several examples of ^{57}Fe spectra for interface sites are shown in Fig. 1. Spectrum (a) was taken from an interface of BCC(α-) Fe contacting with polycrystalline V metal. The sample was a multilayer prepared in ultrahigh vacuum (UHV) by repeating the depositions of the following structure n times on a polyimid substrate: [^{56}Fe(100 Å)/^{57}Fe(3.5 Å)/V]xn. If the surface of the ^{56}Fe layer was ideally flat and no diffusion had taken place, the spectrum would indicate the situation of approximately two topmost interface atomic layers. However, the obtained spectrum is very broad in comparison with a normal 6-line pattern (Zeeman sextet) of α-Fe, suggesting that the hyperfine field is considerably distributed [5]. From the analysis of the hyperfine field distribution $P(B_{hf})$, the range of mixing between Fe and V at the interface is estimated to be not more than three atomic layers [6]. This conclusion is consistent with the analysis of the ^{51}V hyperfine-field distribution observed by NMR [7]. For comparison, a spectrum of the BCC interface in contact with Mg metal, [^{56}Fe(100 Å)/^{57}Fe(3.5 Å)/Mg], is shown in Fig. 1(b) [8]. The spectrum of the Fe/Mg interface shows a more clearly

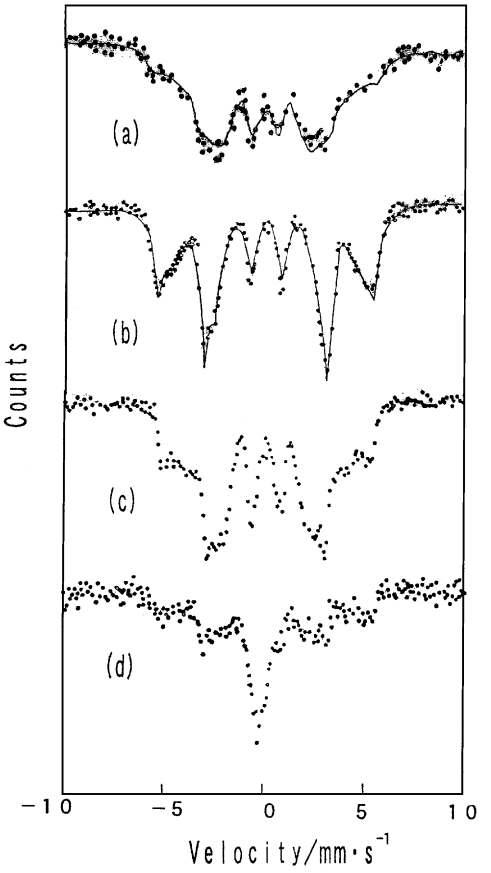

Fig. 1. ^{57}Fe Mössbauer absorption spectra for Fe interfaces covered by various metals: (a) [^{56}Fe(100 Å)/^{57}Fe(3.5 Å)/V] at 4.2 K; (b) [^{56}Fe(1 0 0 Å)/^{57}Fe(3.5 Å)/Mg] at 4.2 K; (c) [^{56}Fe/^{57}Fe/Mn] at 300 K; (d) [Mn/^{57}Fe/^{56}Fe]Mn at 300 K.

resolved 6-line pattern than that of Fe/V, suggesting that the degree of mixing is significantly less. The condition of Fe/Mg interface preparation was almost the same as that of Fe/V but the modification of the interface structure is moderate in the Fe/Mg. Since Fe and Mg are insoluble with each other in the equilibrium state, it seems reasonable that the reactivity at the interface is limited. The interface reactivity thus depends greatly on the combination of elements. Moreover, the structure depends on the procedure of deposition, if the reactivity is relatively high. As an example, the spectra for two kinds of Fe/Mn interfaces are shown in Fig. 1(c) and (d), respectively [9]. The former is a spectrum for an Fe interface covered by a Mn layer (Mn-on-Fe). The line profile is similar to that of the Fe/V interface, but the degree of intermixing is supposed to be somewhat less than the Fe/V case. In contrast, the spectrum for another kind of Fe/Mn interface, where the ^{57}Fe probing layer was deposited on the surface of Mn prior to the thick ^{56}Fe deposition (Fe-on-Mn), was found to be considerably different. The spectrum includes a central line corresponding to a fairly large non-magnetic fraction of Fe atoms, which means diffusion of Fe atoms into Mn layers for more that several atomic layers. The extent of mixing at an interface depends greatly on the procedure of sample preparation. In a multilayer structure built by successive depositions, it can happen that the structures at the top and bottom interfaces of each layer are different, and then the compositional modulation has a unidirectional profile with respect to the film growth direction. Thus, the degree of intermixing may be estimated sensitively by analyzing the hyperfine field distribution observed by ^{57}Fe Mössbauer spectroscopy. A Mössbauer analysis of epitaxially grown Fe/Ag interfaces has been reported by Schurer et al. [10,11].

An issue derived from GMR studies is the relation between spin-dependent scattering probability and interface roughness. It is indeed interesting to apply the Mössbauer techniques to this problem, and already several arguments have been presented [12]. However, the results are not consistent with each other and the optimum interface condition for the enhancement of spin-dependent scattering is not clarified yet. Mössbauer spectroscopy gives us information on the degree of intermixing, that is, the interface roughness on the most microscopic (atomic) scale. In actual interfaces, there exists roughness of various scales. For the estimation of roughness on a macroscopic scale, X-ray techniques are useful. However, if one attempts to prepare samples with different roughness, it is unavoidable that many factors change simultaneously and GMR properties cannot be expressed as a function of a single parameter of roughness. Therefore the relation between roughness and spin-dependent scattering probability remains a matter of debate. Recently, Schad et al. [13] reported that the magnitude of the GMR effect in MBE grown epitaxial Fe/Cr(0 0 1) superlattices depends on both the vertical roughness amplitude η (as obtained from synchrotron X-ray diffraction, XRD) and the lateral roughness, i.e. the step density n_{step} (as determined from CEMS). A linear increase of the GMR with the product, $\eta \times n_{\mathrm{step}}$, was found. This result is based on the model by Landes et al. [14] and Klinkhammer et al. [15] (which is supported by calculations [16,17]), where the hyperfine fields of the components of the CEMS spectra are characteristic for ^{57}Fe probe atoms on different sites at the interfaces or inside the bulk of the layers. Based on this model, the intensities of the spectral components observed in Ref. [13] were assigned to the abundances of the respective ^{57}Fe site as follows: (i) 33 T to bulk positions (n_{bulk}), (ii) 29 and 25 T to sites at interface steps (n_{step}), and (iii) 19 T to sites at atomically flat interface parts (n_{flat}). A reduced ground-state hyperfine field of 25.8 T for the first Fe layer at the flat interface was also observed for Fe(1 1 0)/Cr(1 1 0) sandwiches [18]. The model by Landes et al. [14] is also supported by CEMS results on sputtered Fe/Cr multilayers [19,20].

In Ref. [13] the type of the interfaces, Cr-on-Fe (upper) or Fe-on-Cr (lower), could not be distinguished, but were assumed to be the same. Our CEMS spectra in Fig. 2 demonstrate, however, that the structure of both interfaces is remarkably different. The CEMS spectra in Fig. 2 were measured on epitaxial Fe/Cr(0 0 1) superlattices including two monolayers (ML) thick ^{57}Fe-interface probe layers grown in UHV on MgO(0 0 1) at $T_s = 433$ K. The composition was MgO(0 0 1)/Cr(50 Å)/[$^{\mathrm{nat}}$Fe(12 ML)/^{57}Fe(2 ML)/Cr(8ML)] × 15 (upper)

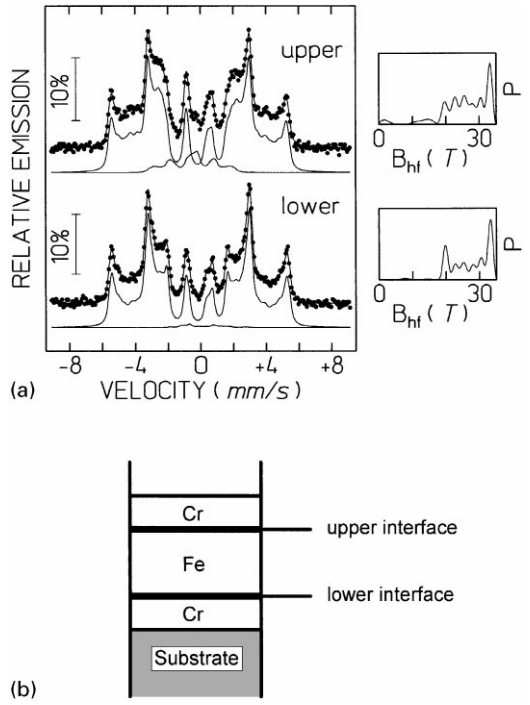

Fig. 2. Room-temperature CEMS spectra from epitaxial Fe/Cr(0 0 1) superlattices on MgO(0 0 1), MBE-grown at $T_s = 433$ K, including 2 ML thick ^{57}Fe-probe layers located either at the upper (Cr-on-Fe) or at the lower (Fe-on-Cr) interfaces. Right-hand side: corresponding hyperfine-field distributions, $P(B_{hf})$. (b) explains the meaning of "upper" and "lower" interfaces.

and MgO(0 0 1)/Cr(50 Å)/[^{57}Fe(2 ML)/^{nat}Fe(12 ML)/Cr(8 ML)] × 15 (lower) (^{nat}Fe = Fe metal of natural ^{57}Fe abundance, 2.1%). The CEMS spectra as well as the corresponding distribution of hyperfine fields, $P(B_{hf})$ of both samples are very different (Fig. 2). The relative areas (relative intensities) of the various peaks observed in $P(B_{hf})$ correspond to the relative abundances of different ^{57}Fe sites at and near to interfaces. The main peak at 33 T determines n_{bulk}, which corresponds to 30% (22%) in relative intensity for the lower (upper) interface. Thus, there are more ^{57}Fe atoms sensing *no* Cr atoms in the lower interface. The peak at 19.6 T (which according to Ref. [13] determines n_{flat}) has a much larger relative intensity for the lower (21%) than for the upper (16%) interface. Moreover, there is a higher $P(B_{hf})$ intensity at lower hyperfine fields (below ~ 18 T) for the upper (5%) than for the lower (1%) interface. Such low B_{hf} values indicate ^{57}Fe atoms with many Cr-neighboring atoms, i.e. some Fe–Cr intermixing. All of these reasons make us to conclude that the lower interface is atomically flatter and shows much less interdiffusion than the upper interface. This agrees with observations by Heinrich et al. [21] and Davies et al. [22] for growth of Cr on Fe.

The interfaces described so far are *real* interfaces in the sense that they are not ideally sharp but exhibit a certain degree of defects, interdiffusion, etc. From the theoretical side, the magnetic and electronic properties of *ideally sharp* interfaces have been the subject of advanced ab initio band structure calculations which allow to compute from first principles the local spin and charge density in thin films of several atomic layers including their surface or interface atomic layer. From the spin density the magnetic moment per atom and the magnetic hf field can be obtained. In particular, Freeman and his group [23] have systematically performed computations of electronic and magnetic properties (including magnetic hf fields) of thin films and ideal interfaces, based on the full potential linearized augmented plane wave (FLAPW) method. Particularly, important is their theoretical discovery [23] that the proportionality between local moment, μ, and hf field, B_{hf}, can fail at ideally flat surfaces and interfaces, contrary to the situation in the bulk. Famous examples are the calculated *enhancement* (relative to bulk values) of the magnetic moment in the first monolayer of free BCC-Fe(1 0 0) surfaces (of 31% [24]) and of free BCC-Fe(1 1 0) surfaces (of 19% [25]). By contrast, the calculated hf fields in the surface layer are *reduced* by 31% for Fe(1 0 0) [24] and by 7.4% for Fe(1 1 0) [25]. This discrepancy was explained [24] by a change in sign of the hf field contribution of the conduction electron polarization at the topmost surface layer. From thin film magnetometry in UHV on free BCC-Fe(1 1 0) surfaces a ground-state surface moment enhancement of 39% has been measured recently [26], which is about twice as large as theory predicts [25]. There is a remarkably good agreement between theoretically predicted and measured reduced surface/interface hf

fields (measured by CEMS) for two systems: (i) for the free BCC-Fe(1 1 0) surface, investigated by Korecki and Gradmann [27], and (ii) for the W(1 1 0)/Fe(1 1 0) interface, measured by Przybylski et al. [28] and calculated by Hong et al. [29]. Details are described in Gradmann's review [30]. An excellent extensive review of CEMS investigations, e.g., on epitaxial BCC-Fe(1 1 0) interfaces with different metallic overlayers (Cr, Gd, Y), was given by Sauer and Zinn [31].

The concept of atomically flat interfaces used in the theoretical work is realized only in very few systems. The theoretically predicted effects will be suppressed by interface roughness and interdiffusion, which cannot be avoided in many multilayer systems. An example is the Fe/Cu(0 0 1) system, where intermixing (Fe–Cu atomic site exchange processes) within the first Cu/Fe interface layer is known to occur [32]. For ferromagnetic 2 ML Fe on Cu(0 0 1), a ground-state surface and subsurface hf field of 24.9 and 31.6 T, respectively, is predicted [33]. Experimentally, a broad distribution of interface hf fields extending from $\sim$12–35 T with an average hf field of $\sim$22 T was observed [34] by CEMS in UHV at 55 K (near magnetic saturation), which is very different from the predicted behavior. As described in Ref. [31], there is also a discrepancy in the hf fields for the Fe/Ag interface, for which a 4% enhancement (with respect to the bulk values) has been observed at low temperature, while calculations predict a 7% reduction. Also in this case interface roughness might play a role. Keavney et al. have studied $[Fe_9(1\,0\,0)/Ag_{40}(1\,0\,0)]_{25}$ multilayers by using a 2-ML ^{57}Fe probe layer [35]. Liu and Gradmann [36] measured Mössbauer spectral parameters of W(0 0 1)/Fe/Ag structures using one ^{57}Fe atomic layer as a probe. Schurer et al. [10] performed a careful and very detailed CEMS analysis of the MBE growth of a 1 ML thick ^{57}Fe probe layer in BCC-Fe(1 0 0)/Ag(1 0 0) structures on a single-crystal Ag(1 0 0) surface. Different Fe sites with different nearest-neighbor (Fe, Ag) configurations at and near the stepped Fe/Ag interface could be observed (e.g., magnetic Fe positions in the central region of terraces, at the edge of the Fe terraces (top or bottom sites), in the first and second subinterface layers, and paramagnetic Fe interface-exchanged with Ag atoms). Mössbauer spectroscopy allowed the determination of the amount of Fe coverage of the substrate and the relative amount of Fe atoms that participate in the atomic Fe-Ag exchange process at the buried Ag/Fe interface [10]. In contrast to the bottom (Fe-on-Ag) interface, the top (Ag-on-Fe) interface was found to be very sharp with 90% of the 1-ML ^{57}Fe-probe atoms at the interface making direct contact with the Ag overlayer. The magnitude of the hf field was found to be 27.6 T at 300 K for Fe in flat terrace sites [10], which is significantly smaller than the BCC-Fe bulk value at 300 K. Unfortunately, Schurer et al. [10,11] could not measure the hf field at low temperature; therefore, a reliable comparison with the calculated ground-state hf field at the Fe/Ag interface [23] is not yet possible.

2.2. *Metastable ultrathin films*: *FCC*-Fe *and* *FCC*-$Ni_{1-x}Fe_x$ *invar*

A vast number of reports on the magnetic and structural properties of the FCC-Fe/Cu(0 0 1) system is found in the literature [37–39]. FCC-Fe does not exist in bulk form at low temperatures. Epitaxy offers the possibility to stabilize crystallographic phases which do not exist as bulk materials under normal conditions. As FCC-Fe is lattice matched to a Cu substrate with a small misfit of $\sim$0.7% only, the structure and magnetic properties of metastable epitaxial FCC-Fe ultrathin films on Cu(0 0 1) have become the subject of numerous investigations. The reason for the general interest in this system is its delicate interplay between structure and magnetism [40], with magnetism being sensitive to changes in the lattice parameter (or Wigner–Seitz radius). So far the majority of investigations was performed on MBE grown FCC-Fe/Cu(0 0 1); recently, however, intriguing new properties of the FCC-Fe/Cu system prepared by pulsed laser-deposition (PLD) have been reported [41,42]. Moreover, FCC-Fe ultrathin films have been stabilized on diamond C(0 0 1) [43] and $Cu_{86}Al_{14}$(0 0 1) substrates [44]. During the 30 years of research on MBE-grown FCC-Fe/Cu(0 0 1) films after the discovery of epitaxy for this system [45,46] many seemingly contradictory experimental results have been reported in the literature. However, in the past years a complex

structural and magnetic "phase diagram" (with film thickness t and growth temperature T_s as parameters) has been suggested [47,48] for MBE grown FCC-Fe/Cu(0 0 1) which (at least for room-temperature growth, $T_s \approx 300$ K) is now widely accepted and has been confirmed by various experimental methods, including in situ CEMS in UHV [37]. It is generally accepted that such Fe films on Cu(0 0 1) prepared at $T_s \approx 300$ K in the 2–4 ML thickness range are ferromagnetic (FM) with a high Fe magnetic moment of $\sim 2\ \mu_B$ (and with a large saturation hyperfine (hf) field of ~ 31–34 T [37], accidentally similar to that of BCC-Fe), and posses the fct structure, including some vertical and lateral 'buckling' of Fe atoms [49,50]. Moreover, for Fe on Cu(0 0 1) prepared at $T_s \approx 300$ K in the ~ 5–10 ML range, the interior of the films shows the undistorted FCC structure, is paramagnetic at RT and antiferromagnetic (AFM) with a low magnetic moment (~ 0.5–$0.7\ \mu_B$) and low hf field of ~ 1–2 T at low temperature, while ferromagnetism is restricted to the film-vacuum surface region, where surface-atom positions relax towards a local FCT structure [49,50].

Site-selective (^{57}Fe-probe layer) CEMS provided the first *direct* observation of surface-restricted magnetic order and paramagnetism in the interior of 300 K grown 7 ML Fe films on Cu(0 0 1) [37]. This is demonstrated in Fig. 3 where site-selective CEMS spectra of 2 ML thick ^{57}Fe-probe layers in otherwise natural Fe/Cu(0 0 1) films (of 7 ML total thickness) are shown: The ^{57}Fe-probe layer was deposited either on top of the film (upper spectrum), in the film center (center spectrum) or at the Fe/Cu(0 0 1) interface (bottom spectrum). At the surface the dominant spectral contribution involves a broad distribution of magnetic hyperfine fields, $P(B_{hf})$, with an average field $\langle B_{hf} \rangle$ of ~ 18 T. Obviously, the large majority of the ^{57}Fe nuclei at the film surface experiences high B_{hf} values ranging from ~ 10 to ~ 35 T at 300 K; hence these Fe atoms are in a probably ferromagnetic high-moment (or high-spin, HS) state. The distribution $P(B_{hf})$ of the surface does *not* appear in the center or at the Fe/Cu interface (Fig. 3), i.e. the spectrum of the film center and of the Fe/Cu interface do not exhibit a magnetic component at 300 K. Instead, a dominant sharp central single line due to paramagnetic (undistorted) FCC-Fe appears at 300 K, superimposed to a (less intense) asymmetrical quadrupole-split doublet of splitting $\Delta E_Q = 0.63$ mm/s. The relative spectral intensity of the doublet is clearly enhanced when the ^{57}Fe-probe layer is placed at the Fe/Cu interface as compared to the film center (Fig. 3). Therefore, the quadrupole doublet was assigned to the Fe/Cu(0 0 1) interface (which is paramagnetic at 300 K), where the electronic charge distribution is anisotropic and gives rise to an electric field gradient at the ^{57}Fe nucleus. It is observed that the relative doublet intensity amounts to 43% of the total spectral intensity at the interface; this means that effectively 0.86 ML of

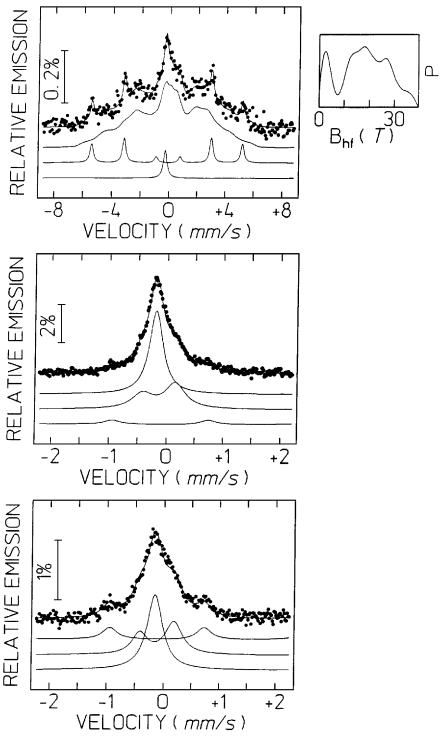

Fig. 3. Site-selective CEMS spectra at 300 K of room-temperature grown ^{57}Fe probe layers in natural FCC-Fe/Cu(0 0 1): ^{57}Fe(2 ML)/^{nat}Fe(5 ML)/Cu(0 0 1) (top); ^{nat}Fe(2 ML)/^{57}Fe(3 ML)/^{nat}Fe(2 ML)/Cu(0 0 1) (center); and ^{nat}Fe(5 ML)/^{57}Fe(2 ML)/Cu(0 0 1) (bottom). [The sharp sextet subspectrum (top) and the two lines at -0.9 and $+0.7$ mm/s (center and bottom) are an artifact due to the α-Fe coated sample-holder frame in this case]. Notice the different velocity scale (top). (From ref. [37]).

the (in total) 2 ML thick ^{57}Fe-probe layer at the Fe/Cu interface sense the influence of Cu atoms, implying that the chemical roughness of the Fe/Cu interface is limited to $\sim$ 1 ML Fe only [37].

Since the development of a magnetic hyperfine field upon cooling below the magnetic ordering temperature is independent of the type of magnetic ordering (regardless whether ferromagnetic or antiferromagnetic), Mössbauer spectroscopy is presently the only technique with monatomic layer sensitivity for determining the Néel temperature, T_N, of AFM FCC-Fe films in the $\sim$ 5–10 ML range [37,51]. The FCC-Fe single line broadens considerably in the AFM state at low temperatures due to the unresolved magnetic hyperfine splitting in the AFM phase [37,51–53]. The average saturation hyperfine field observed in the AFM FCC-Fe state is $\sim$ 1-2 T as compared to the natural linewidth of $\sim$ 0.8 T for ^{57}Fe. This low hyperfine field indicates that AFM FCC-Fe films are in a low moment (low-spin, LS) state. The onset of line broadening upon cooling determines the Néel temperature, as demonstrated in Fig. 4 for a $\sim$ 5 ML thick FCC-Fe film on an atomically flat well-ordered Cu(0 0 1) surface with $T_N \sim 70$ K. For comparison, the single line of a $\sim$ 5 ML FCC-Fe film grown at 300 K on a $Cu_{86}Al_{14}$(0 0 1) single-crystal surface with an expanded lattice parameter (1.6% relative to that of Cu) does not show significant line broadening upon cooling down to 35 K (Fig. 4) [34]. Therefore, T_N of FCC-Fe/$Cu_{86}Al_{14}$(0 0 1) is considerably reduced ($T_N \leqslant 35$ K), as compared to FCC-Fe/Cu(0 0 1). The reason might be the expanded $Cu_{86}Al_{14}$ lattice, although the effect of possible Al impurities in the FCC-Fe film cannot be excluded [34].

A plot of the saturation hyperfine field B_{hf} versus the Wigner–Seitz radius r_{ws} (in atomic units) for different FCC-like Fe system is shown in Fig. 5 [34] (Note that $r_{ws} = 2.67$ a.u. for Cu). As B_{hf} is roughly proportional to the local Fe magnetic moment, Fig. 5 reflects also the behavior of the local moment versus r_{ws}. Thus Fig. 5 demonstrates that there is a transition from an AFM low-spin Fe state to a FM high-spin Fe state around $r_{ws} \sim 2.69$ a.u., which is in agreement with theoretical predictions for bulk FCC-Fe [40]. In Fig. 5 also data for ultrathin FCC-Fe-like films on Cu_3Au(0 0 1) [54],

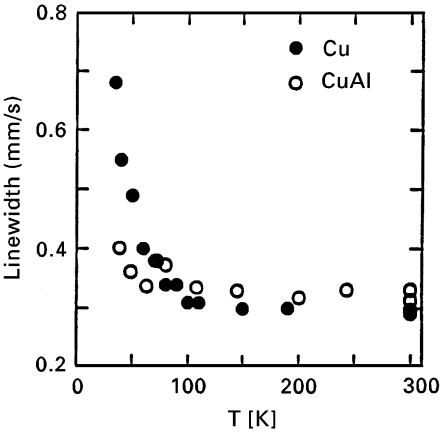

Fig. 4. The FCC-Fe linewidth (FWHM) vs temperature for $\sim$ 5 ML ^{57}Fe grown at 300 K on Cu(0 0 1) (full circles) and on $Cu_{86}Al_{14}$(0 0 1) (open circles). (From ref. [34]).

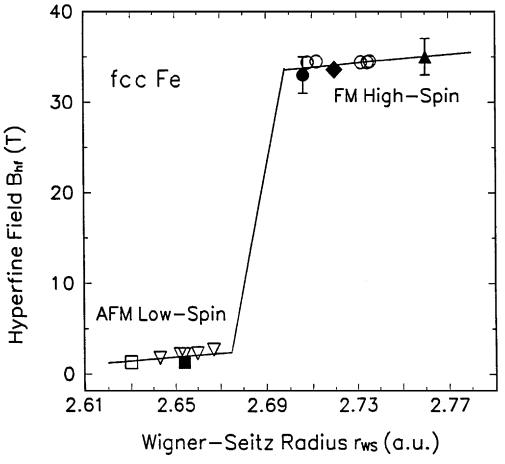

Fig. 5. Hyperfine field near magnetic saturation vs Wigner-Seitz radius, r_{ws}, for FCC-Fe-like systems [34]: Full square: 300 K grown 5-10 ML FCC-Fe/Cu(0 0 1) measured at 35 K. Full circle: 300 K or 100 K grown 3 ML thick Fe/Cu(0 0 1) and 100 K grown 7 ML thick Fe/Cu(0 0 1), measured at 40–55 K. Full triangle: 300 K grown 5 ML thick Fe/Cu_3Au(0 0 1), measured at 30 K [54]. Open circles: 275 K grown Fe/$Cu_{1-x}Au_x$(0 0 1) multilayers, measured at 15 K [55]. Open triangles: Fe precipitates in bulk $Cu_{100-x}Al_x$ matrices, measured at 4.2 K [54]). Open square: Fe precipitates in bulk $Cu_{86}Al_{14}$ matrix at 58 kbar pressure, measured at 4.2 K (cited in ref. [54]). Full diamond: 475 K grown hcp Fe/Ru(0 0 0 1) superlattice, measured at 4.2 K [56].

FCC-like Fe/$Cu_{1-x}Au_x$(0 0 1) multilayers [55], and for FM HCP-Fe/Ru(0 0 0 1) superlattices [56] are included; furthermore, data from AFM FCC-Fe precipitates in $Cu_{100-x}Al_x$ matrices have been added in Fig. 5 [54]. These results represent quite well the trends found in theoretical hf fields for bulk FCC-Fe by Herper et al. [57], calculated by the method of Blügel et al. [58]. The hf fields calculated by the embedded cluster method for FCC-Fe with a simple AFM spin structure [59] deviate considerably from those in Ref. [57].

The magnetic and structural properties of FCC-Fe are related to the Invar effect [60], i.e., anomalies in thermal expansion and other physical properties of Fe-based FCC alloys, for instance, FCC-$Ni_{1-x}Fe_x$ alloys near $x = 0.65$. According to Weiss' phenomenological model [61], the Invar effect originates from thermal transitions between a ferromagnetic (FM) high-spin Fe *state* with a large atomic volume and an energetically higher lying antiferromagnetic (AFM) low-spin Fe *state* with a small atomic volume. Indeed, modern electronic band-structure calculations of the magnetic ground state in bulk Ni–Fe Invar alloys predicted the existence of these two Fe states [62–64]. Experimentally, in bulk FCC-$Ni_{1-x}Fe_x$ alloys, the study of the region of high Fe concentration is hampered by the onset of a structural phase transition to the BCC-Ni–Fe phase (martensitic transformation). In epitaxial FCC-$Ni_{1-x}Fe_x$ films, however, the martensitic transformation can be suppressed by pseudomorphic growth on Cu substrates over the entire Fe concentration range [65,66]. Walker and his group [67] investigated epitaxial FCC-$Ni_{1-x}Fe_x$ alloy thin films on Cu(0 0 1) and Cu(111) utilizing a combination of Mössbauer spectroscopy and magnetometry; their results presented clear evidence for the emergence of a low-spin AFM *phase* in the region of high Fe content (Invar region), which coexists with a high-spin FM *phase* [67]. The emergence of the AFM phase was observed by magnetometry as a drop in the average saturation moment, while low-temperature Mössbauer spectroscopy revealed the emergence of this phase by the appearance of a drastically broadened central single-line superimposed to the sextet of the high-spin FM phase. The high-spin FM phase may exist as superparamagnetic clusters in a matrix of the low-spin AFM phase that was found to have a Néel temperature around 35 K. Apparently, the AFM phase is invisible for SQUID magnetometry, and the average magnetization drops, as more of the AFM phase emerges with increasing Fe concentration [67].

It is tempting to investigate FCC-Fe films grown pseudomorphically on substrates with different expanded lattice parameters in order to scan the in-plane lattice parameter around its value for the magneto-volume instability (low-spin/high-spin transition) described above (Fig. 5). This may be performed e.g., by choosing $Cu_{1-x}Au_x$ substrates which show an increasing lattice parameter with rising Au concentration [55,68,69]. A Mössbauer-effect study by Keavney et al. [55] of FCC-Fe(1 0 0)/$Cu_{1-x}Au_x$(1 0 0) multilayers with lattice parameters in the range between 3.606 and 3.704 Å demonstrated the *coexistence* of the low-spin AFM and the high-spin FM Fe phase. Most interestingly, the hyperfine fields (and the local Fe atomic moments) themselves of these two Fe sites do *not* change, respectively, with the substrate lattice parameter, but it is the population of the high-spin FM phase that was found to increase relative to that of the low-spin phase, as the lattice parameter of the substrate is increased [55]. This effect causes the continuous increase in the *average* moment per Fe atom [55,68,69], as measured by macroscopic magnetometry. Remarkably, hyperfine fields (or Fe atomic moments) in FCC-Fe intermediate between those of the low-spin AFM and high-spin FM FCC-Fe phases (see Fig. 5) have never been observed convincingly, which probably indicates a first-order transition between these two phases, as predicted by theory [40].

2.3. Perpendicular spin structures

For the studies of magnetism in thin films, the direction of spontaneous magnetization is a valuable information. If the shape anisotropy is dominant, the magnetization is preferably oriented in the film plane. However, it is not uncommon to observe an off-plane component of magnetization. Films having perpendicular magnetizations are of interest from viewpoints of basic magnetism and also of technical applications. The average spin

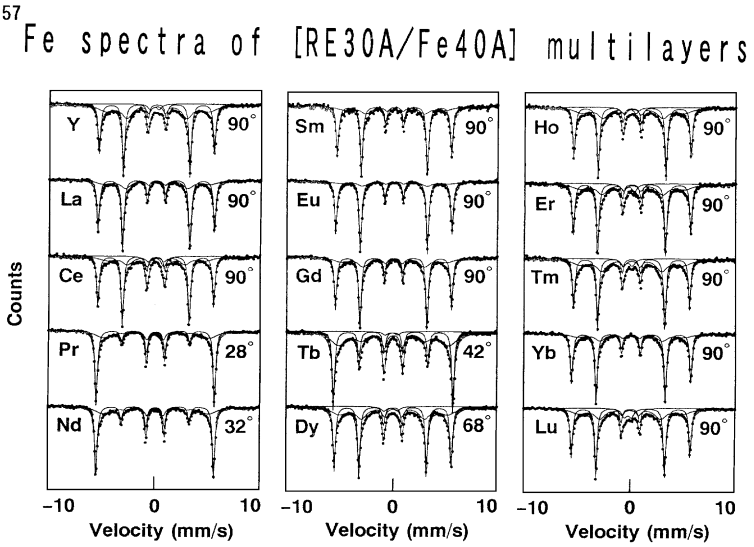

Fig. 6. ^{57}Fe Mössbauer absorption spectra at 4.2 K for [Fe(40 Å)/RE(30 Å)] multilayers (RE = rare earth). The average direction $\langle\Theta\rangle$ of the Fe magnetic moments relative to the film normal is shown for each spectrum.

direction is easily estimated from the Mössbauer hyperfine spectra. The intensity ratio of six lines in a magnetically split ^{57}Fe spectrum is expressed as $3 : x : 1 : 1 : x : 3$ and $\cos^2\Theta = (4 - x)/(4 + x)$, where Θ is the polar angle between the direction of the Fe magnetic moment and the γ-ray beam (i.e. the film normal). The measured values of $\cos^2\Theta$ are spatial averages of $\langle\cos^2\Theta\rangle$ over the Fe layers. Usually, a half-cone angle $\langle\Theta\rangle$ is defined by arccos $(\langle\cos^2\Theta\rangle)^{1/2}$. In a powder pattern with random spin orientation, the ratio is 3 : 2 : 1 : 1 : 2 : 3, but in the case of perfect perpendicular (in-plane) magnetization, the ratio becomes 3 : 0 : 1 : 1 : 0 : 3 (3 : 4 : 1 : 1 : 4 : 3). As examples, spectra for Fe/rare-earth multilayers are shown in Fig. 6 [70]. It is observed that the ratio for the most cases is 3 : 4 : 1 : 1 : 4 : 3, indicating the magnetization being in the plane. However, the intensity ratios in the spectra for Pr, Nd and Tb are different, suggesting the magnetization is oriented close to the film normal. Although all the samples with the same nominal structure were prepared in the same procedure, and have similar crystallographic qualities, the effective anisotropies of Fe layers are different, depending on the counterpart rare-earth elements. The reason is attributed to the orbital angular momentum of interface rare-earth atoms.

Nanoscale chemically modulated Tb/Fe and other RE/Fe multilayers with rather thin individual layer thickness ($< \sim 20$ Å) have been extensively investigated, mainly because they may exhibit perpendicular magnetic anisotropy at room temperature [71]. RE/Fe multilayers (in particular Tb/Fe, Dy/Fe) with thicker individual layer thicknesses ($> \sim 26$ Å) have crystalline HCP/BCC structure and may show a reversible temperature-driven Fe-spin reorientation transition $\langle\Theta\rangle$(T) from parallel to perpendicular spin orientation upon cooling. This phenomenon has been discovered by ^{57}Fe Mössbauer spectroscopy in HCP-Dy/BCC-Fe multilayers for the first time [72], and was later studied in other HCP-RE/BCC-Fe systems [70,73], and also by ^{161}Dy Mössbauer spectroscopy [74]. Spin-reorientation transitions are of fundamental interest because of the competing magnetic interactions involved [75,76]. Since the interface roughness plays an important role in the origin of perpendicular magnetic anisotropy, Tb/BCC-Fe multilayers have been ion-beam irradiated with heavy ions in order to modify the interface and BCC-Fe structure by demixing, mixing and

amorphization [77–79]. Depending on the type of ions and the irradiation dose employed enhancement or reduction of the perpendicular Fe-spin orientation was observed by CEMS.

2.4. Magnetization process and domain structure

Fe-site-selective detection of magnetic domains and calculation of an Fe-specific magnetic hysteresis loop generally may be achieved by Mössbauer spectroscopy in an external field, B_{ext}, in such cases where the coercivity B_c is larger than the experimental linewidth $\Gamma \approx 0.8$ T, and the system shows a strong uniaxial magnetic anisotropy. This applies in particular to Fe-containing modern hard-magnet systems either as thin-film/multilayer or bulk materials. This is demonstrated for HCP-Tb/BCC-Fe multilayers at 50 K, where they exhibit strong perpendicular magnetic anisotropy and $B_c \approx 1.2$ T [80]. Similar results have been obtained at 4.2 K [80]. Polycrystalline HCP-Tb/BCC-Fe multilayers of composition [^{nat}Fe(17.5 Å)/^{57}Fe(5 Å)/^{nat}Fe(17.5 Å)/Tb(26 Å)] × 30 and capped by Al(50Å) were prepared by thermal evaporation of high-purity elements in UHV ($p \leqslant 3 \times 10^{-9}$ mbar during deposition, rate 0.2 Å/s) onto liquid-nitrogen cooled polyimid (Kapton) substrates for Mössbauer transmission experiments. The Mössbauer signal from the natural Fe layers (^{nat}Fe) is negligible, and the signal arises essentially from the center of the BCC-Fe layers. Thus we avoid possible spectral contributions from intermixed interface regions [81,82]. Low-angle XRD patterns of our multilayers typically exhibited four or more superstructure Bragg peaks [83] indicating good layer quality. Mössbauer transmission experiments were performed at 50 K in external fields of $-5\ \text{T} \leqslant B_{ext} \leqslant +5$ T parallel or antiparallel to the γ-ray direction and to the film normal.

Typical Mössbauer spectra measured along a hysteresis loop at different fields from $B_{ext} = +5$ to -4 T and back to $+1.5$ T are shown in Fig. 7. As expected, at remanence ($B_{ext} = 0$) and at saturation ($B_{ext} = +5$ T) only one magnetically split sextet with sharp lines typical for BCC-Fe is observed; the sample is in a single-domain state in this case. From the line-intensity ratio a half-cone angle $\langle\Theta\rangle$ of 26° is obtained at remanence, i.e. the average Fe-spin orientation is strongly (but not completely) perpendicular to the plane in the *center* of the BCC-Fe layers. Even at saturation ($+5$ T) a finite angle $\langle\Theta\rangle$ of 22° remains. At $B_{ext} = +1.5$ T, a splitting into two sextets with sharp lines and with different 'effective' field values, $|B_{eff}^{\pm}|$, are observed, representative of 'up' domains (+) and "down" domains (−) respectively, of the perpendicular multidomain state. The reason for the splitting is the vectorial relation $B_{eff} = B_{hf} + B_{ext}$ between the measured effective field at the ^{57}Fe nucleus, the intrinsic hyperfine field, B_{hf}, and B_{ext}. As B_{hf} is related to μ_{Fe} by $B_{hf} = A\mu_{Fe}$ (where

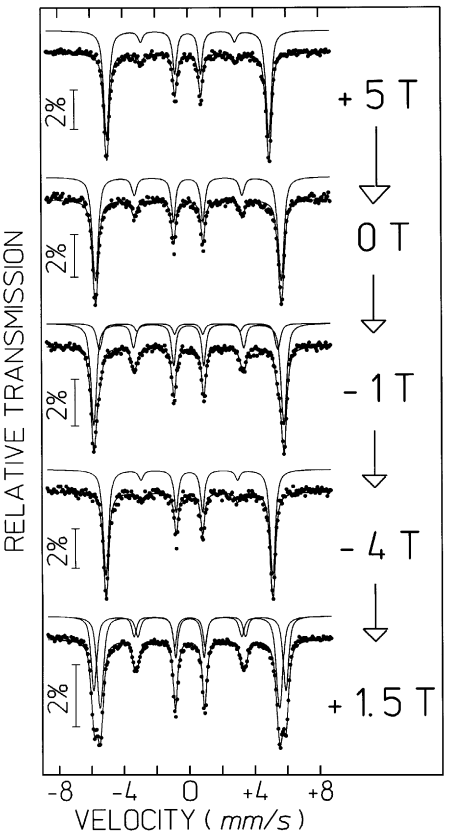

Fig. 7. ^{57}Fe(5 Å)-probe layer Mössbauer spectra of [Tb(26 Å)/Fe(40 Å)] × 30 measured at 50 K along the hysteresis loop in various perpendicular fields, B_{ext}, in the sequence indicated on the right-hand side. The ^{57}Fe-probe layers are in the center of the 35 Å thick natural Fe layers.

$A = -15\ \mathrm{T}/\mu_B$ for BCC Fe), two different μ_{Fe} orientations (corresponding to 'up' or 'down' domains) with respect to B_{ext} result in the two $|B_{eff}^{\pm}|$ values observed. The relative spectral area (relative intensity) $A^{+}(A^{-})$ of the sextet corresponding to "up" ("down") domains is equal to the Fe-specific volume fraction of these perpendicular domains,

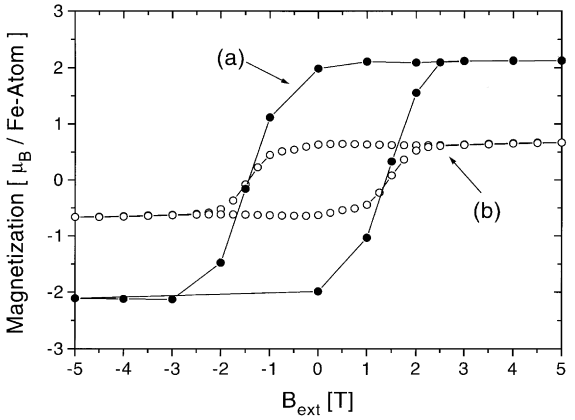

Fig. 8. Perpendicular magnetization loops at 50 K: (a) full circles: Fe site-selective loop calculated from Mössbauer data obtained from Fig. 7. (b) open circles: SQUID magnetization loop [80].

which changes with B_{ext}. This provides the basis for calculating an Fe-specific magnetization hysteresis loop [80] from measured values of $A^{\pm}$, $|B_{eff}^{\pm}|$ and $\cos\langle\Theta\rangle_{\pm}$. The result is shown in Fig. 8, data (a), together with the perpendicular magnetization loop obtained at 50 K from the same sample by SQUID magnetometry (data (b)). Comparison of both curves provides important information: (i) they have about the same coercivity, and (ii) at saturation, the average magnetization in (b) is only 0.7 μ_B/Fe-atom, compared to 2.1 μ_B/Fe-atom in (a); this demonstrates that 1.4 μ_B/Fe-atom are compensated at the Tb/Fe interfaces at 50 K by antiferromagnetic coupling with Tb moments.

If domain structures are formed in a magnetic film in zero external field, the direction of magnetization in a film is not uniform. For example, the direction of magnetization in a closure-domain structure will vary depending on the depth from the surface. Depth-dependent analysis of the magnetization direction using ^{57}Fe probe layers was carried out for a [Co(30 Å)/Au(20 Å)]xn system [84]. For Mössbauer absorption spectroscopy, ^{57}Fe probe layers with a nominal thickness of 1.5 Å were located in the center of 30 Å Co layers at different depths in different samples. As shown in Fig. 9, the

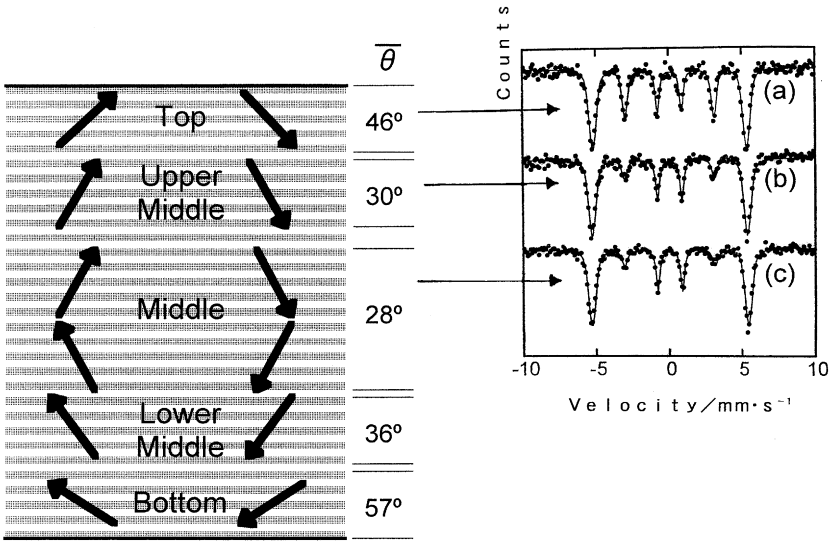

Fig. 9. Concept of magnetic structure in the multilayer system [Co(20 Å)/Au(20 Å)] × 31. Examples of Mössbauer spectra from position-selectively located ^{57}Fe probes are also shown.

line-intensity ratios in the Mössbauer spectra indicate clearly the difference of magnetization directions between the interface and the middle of the multilayer system. The magnetization is closer to the film plane at interface layers and turns towards the perpendicular direction at the inner layers. This result provides evidence for closure domain formation. More details related to the dependence of Mössbauer spectra on the depth from the interface, the number of magnetic layers and on externally applied magnetic fields will be presented in a forthcoming paper.

2.5. *Artificial layered structures*: FePt(0 0 0)$L1_o$ *films*

Thin films of the chemically ordered face-centered tetragonal (FCT) phase of FePt, FePd [85] or (metastable) FeAu [86] with the $L1_o$ structure (or CuAu(I) structure) have become a topical subject. This structure consists of alternating monatomic layers of the elements with the *c*-axis of the FCT unit cell perpendicular to the layers. Epitaxial growth of $L1_o$-ordered FePt thin films on MgO(0 0 1) with the *c*-axis along the film-normal direction by molecular-beam epitaxy (MBE) [87] or magnetron sputtering [88,89] results in high perpendicular magnetic anisotropy. Because of this property and its large magneto-optical Kerr rotation [87], FePt is considered to be a potentially useful storage medium for high-density magneto-optical perpendicular recording.

Mössbauer spectroscopy offers a convenient way to detect the presence of the $L1_o$-phase and of other Fe–Pt phases in this system. For this purpose we have studied 250 Å thick chemically ordered ($L1_o$) $^{57}Fe_{50}Pt_{50}$ alloy films and $[^{57}Fe(1.5\ Å)/Pt(2.0\ Å)]_{60}$ superlattices grown by MBE at 500°C on MgO(0 0 1). Initially, the MgO(0 0 1) surface was covered at 500°C by a 3 Å ^{57}Fe seed layer followed by a 150 Å Pt(0 0 1) buffer layer. All samples were capped with 10 Å Pt at 500°C for protection. High-angle XRD patterns exhibited clear FePt(0 0 1)- and (0 0 3) Bragg reflections from the $L1_o$ superstructure, in addition to the basic FePt(0 0 2) and (0 0 4) Bragg peaks, typical for epitaxial growth. Similar multilayers prepared without Fe-seed layer, however, did not grow epitaxially, but showed a clear FePt(1 1 1) texture.

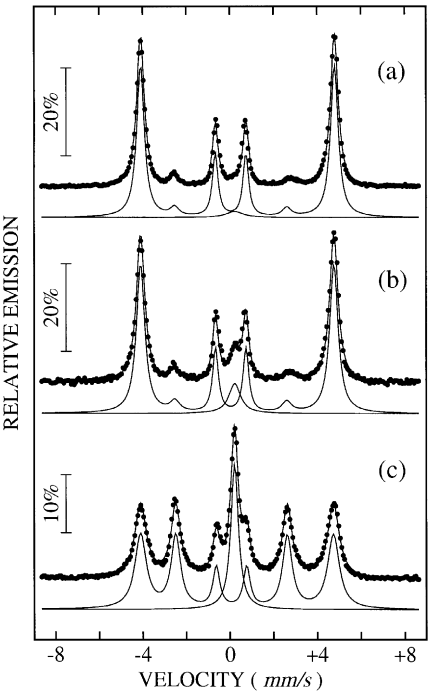

Fig. 10. CEMS spectra of $L1_o$-ordered $^{57}Fe_{50}Pt_{50}$ systems at 300 K: (a) 250 Å epitaxial $^{57}Fe_{50}Pt_{50}$(0 0 1) alloy film. (b) Epitaxial (0 0 1)-oriented $[^{57}Fe(1.5\ Å)/Pt(2.0\ Å)] \times 60$ superlattice. (c) (1 1 1)-textured (non-epitaxial) $[^{57}Fe(1.5\ Å)/Pt(2.0\ Å)]_{80}$ multilayer grown without ^{57}Fe(3 Å) seed layer.

Fig. 10 shows the CEMS spectra of the Fe–Pt samples measured at room temperature. The incident gamma radiation was perpendicular to the film plane. All spectra in Fig. 10(a)–(c) could be analyzed in terms of a dominant magnetically split Zeeman sextet with slightly asymmetric line positions which is assigned to the epitaxial (FCT) FePt phase with $L1_o$ structure, and a less-intense central single line due to some cubic non-magnetic (minority) Fe–Pt phase. The relative spectral intensity of this non-magnetic phase amounts to 3.2% of the total spectral intensity in Fig. 10(a), 9.3% in Fig. 10(b) and increases to 23.2% in Fig. 10(c). The non-magnetic Fe–Pt phase was found to order magnetically at low temperature with a hyperfine field different from that of the $L1_o$ phase.

Spectral analysis yields an average hyperfine field of 27.5 T for the FCT ($L1_o$-ordered) FePt phase at RT. The outer sextet lines are slightly broader than the inner lines, in particular in the case of the (1 1 1) textured film (Fig. 10(c)). This is the result of a distribution of hyperfine fields (which is relatively narrow and sharply peaked, though). The $P(B_{hf})$ distribution reflects small deviations from the ideal short-range-order parameter of the perfect $L1_o$ phase. The latter has one unique Fe-lattice site only, and thus should show a sharp B_{hf} value and no distribution. From the relative line intensities of the spectra in Fig. 10(a) and (b) a tilting angle $\langle\Theta\rangle$ of $\sim 19°$–$21°$, i.e. nearly complete perpendicular Fe-spin orientation, was obtained for the epitaxial films. The angle $\langle\Theta\rangle$ deduced from Fig. 10(c) is 60° for the (1 1 1)-textured multilayer. This is close to the angle of 54.7° between the preferred crystallographic $\langle 1\,1\,1\rangle$ direction along the film normal and the tilted c-axis directions in this textured system.

The non-cubic (FCT) $L1_o$ structure with its anisotropic electronic charge distribution manifests itself in a strong electric quadrupole interaction with the ^{57}Fe nucleus. This is reflected by asymmetrical line positions in the Zeeman sextet [90]. Spectral analysis combined with the assumption that the main component of the electric field gradient, V_{zz}, is parallel to the tetragonal c-axis, and the asymmetry parameter $\eta = 0$, results in a positive electric quadrupole-coupling constant $eV_{zz}Q/2$ of $+0.36$ mm/s for our epitaxial FCT FePt systems. Ordered ($L1_o$) FCT $Fe_{50}Pd_{50}$ thin-film alloys co-deposited at 600°C show similar values of B_{hf} and $eV_{zz}Q/2$ as our FCT FePt samples [91].

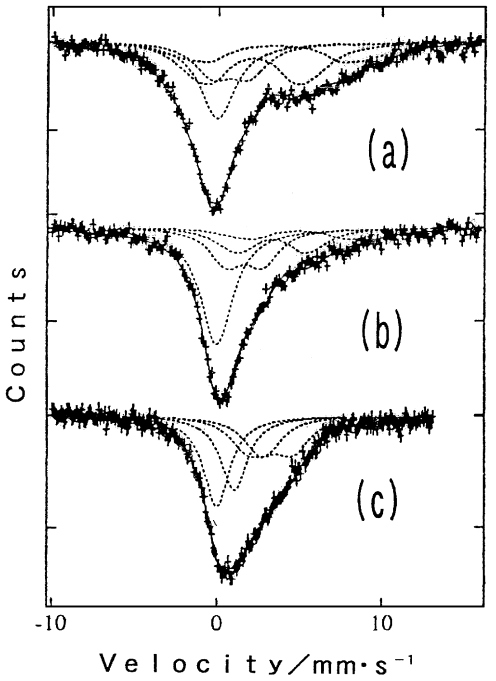

Fig. 11. ^{197}Au Mössbauer spectra of [Au(10 Å)/3d-metal] multilayers at 16 K: (a) [Au(10 Å)/Fe(8 Å)]; (b) [Au(10 Å)/Co(20 Å)]; (c) [Au(10 Å)/Ni(20 Å)].

3. Studies of non-magnetic layers

The GMR effect is a transport phenomenon typically between magnetic layers separated by a non-magnetic spacer layer. It is important to clarify the role of the spacer layer from the viewpoint of magnetism. In order to observe directly the magnetic properties of non-magnetic layers, Mössbauer probes of a non-magnetic element such as ^{197}Au, is useful. Au is very commonly used as a spacer element, as well as Cu, and actually the short-period oscillation of interlayer coupling was first observed in Fe/Au/Fe sandwich films [92].

^{197}Au Mössbauer measurements have been performed by the group of Nasu, Osaka University. Examples of spectra measured at 16 K for several multilayers of Au and ferromagnetic 3D-metals are shown in Fig. 11 [93]. The profiles of the spectra are broad and asymmetric, but can be interpreted as a superposition of two components, a bulk Au-like (non-magnetic) part and a magnetically split one. The relative amount of the latter (magnetic fraction) increases with the reduction of the Au layer thickness, and therefore the magnetic fraction is attributed to the interface part. The hyperfine fields in each Au spectrum are fairly large: 115.0, 69.0 and 23.0 T for the interfaces with Fe, Co and Ni, respectively, suggesting that the spin polarization at the interface Au sites is rather high. The magnitude of the hyperfine field at the interfaces varies corresponding to the magnitude of

magnetization in Fe, Co and Ni. The Au isomer shift is very sensitive to a change of the electronic structure. The observed spectral profile is interpreted by assuming a large positive isomer shift for the part with a large magnetic hyperfine field. The amount of the interface fraction having appreciable hyperfine field values corresponds to less than two monolayers. Probably, the Au atoms exhibiting large hyperfine fields have direct bondings with ferromagnetically polarized 3D orbitals of Fe. It is likely that spin polarization by conduction electrons exists more extensively, but the hyperfine fields at Au nuclei caused by conduction electron polarization seem to be fairly small. In summary, large magnetic polarization at interface Au sites caused by direct coupling with ferromagnetic metals was observed, but more refined measurements with a higher sensitivity are required to detect a conduction electron spin polarization.

It is to be noted that a significant magnetic hyperfine broadening is also observed at interface Au sites in Au/Cr multilayers. This fact means that the Cr interface has a ferromagnetic spin arrangement, although bulk Cr is a compensated antiferromagnet. Further experiments on Au/Cr multilayer systems will be carried out in near future.

Another candidate of nanoprobe for the studies of non-magnetic layers is Sn, since ^{119}Sn is a very convenient Mössbauer isotope, like ^{57}Fe. Magnetic properties of Au layers in Au/3D multilayers including ^{119}Sn probes have been investigated systematically by applying transmission ^{119}Sn Mössbauer spectroscopy. Probing-layers of ^{119}Sn with a nominal thickness of 1.5 Å were inserted in Au layers in Au/3D multilayer samples, and transmission spectra were measured [94]. Fig. 12(b)–(d) shows ^{119}Sn spectra, where the Sn probes were located in the center of Au layers with 20 Å thickness in Au/3D (Fe, Co and Ni) multilayers. All spectra show broadenings caused by magnetic hyperfine fields, suggesting that spin polarization exists at a distance of 10 Å from the interface. For comparison, a spectrum where Sn is at the center of 30 Å Au layers is also shown (Fig. 12(a)) which has almost not broadening. The transferred spin polarization seems to have almost decayed out in the region from 10 to 15 Å.

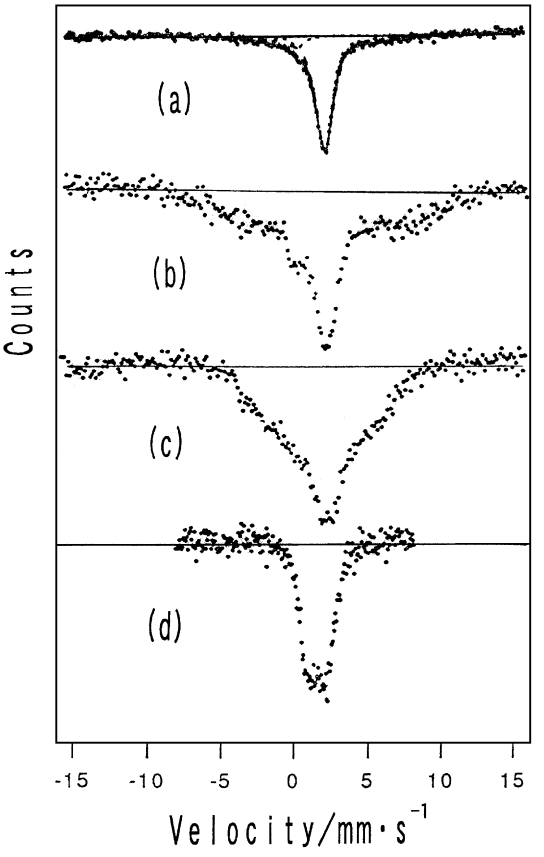

Fig. 12. ^{119}Sn Mössbauer spectra at 300 K of [3d-metal/Au(10 Å)/Sn(1.5 Å)/Au(10 Å)] multilayers: 3d-metal is (b) Co(20 Å), (c) Fe(20 Å), (d) Ni(20 Å). [Au(15 Å)/Sn(1.5 Å)/Au(15 Å)/Co(20 Å)] is shown for comparison in (a).

The Sn probe atoms in Au layers are not isolated impurities, but have an ultrathin layered structure with a nominal thickness of 1.5 Å, corresponding roughly to one Sn monolayer. Crystallographically, the microscopic structure of such a thin Sn layer in Au is not known and the mechanism for the transferred hyperfine field at the Sn nuclear site is not clear. However, as far as the structure of the Sn layers in Au is the same in all the samples, the ^{119}Sn layer is regarded as a probe to measure spin polarization. The observed hyperfine fields at Sn should be proportional to the local spin polarization in Au. The Sn hyperfine field in Au/Ni at 4.2 K is

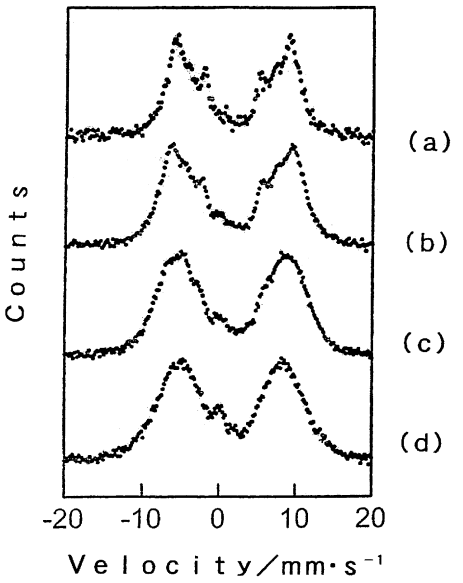

Fig. 13. ^{119}Sn CEMS spectra at 300 K of Cr/Sn multilayers with various Cr thicknesses: (a) $t_{Cr} = 30$ Å; (b) $t_{Cr} = 20$ Å; (c) $t_{Cr} = 10$ Å; (d) $t_{Cr} = 6$ Å.

about 1.0 T, which is smaller than that in Au/Co or Au/Fe, being consistent with the smaller magnetization of Ni. The hyperfine fields in both Au/Fe and Au/Co are fairly large, and the largest value of the hyperfine field in Au/Co at 4.2 K is about 12.0 T, which is larger than that in Au/Fe, about 8.0 T, in contrast to the magnitude of the bulk magnetization. In both cases, hyperfine fields are widely distributed and a considerable fraction has nearly zero hyperfine field. It is plausible that this wide distribution of hyperfine fields originates from an oscillatory spin polarization of conduction electrons in Au layers.

Although there are a number of investigations on the GMR effect in Fe/Cr multilayer systems, it was not clear until recently whether ultrathin Cr layers have a magnetic order or not. Ultrathin Cr layers appeared to have no magnetization, and magnetic order in a Cr spacer layer itself has been ignored in the arguments on GMR. The present systematic study on the transferred hyperfine field at Sn in Au layers contacting with 3D metal layers (see Fig. 12) have not yet been extended to Cr because initially a penetration of spin polarization from Cr layers into Au layer was not excepted. According to the neutron diffraction studies by Sonntag et al. [95], very thin Cr films have a commensurate antiferromagnetic order and the transition temperature is much higher than that of bulk Cr. ^{119}Sn Mössbauer results on Cr/Sn multilayer systems are consistent with their conclusion.

Multilayers consisting of Cr and Sn layers have been prepared, and remarkably large hyperfine fields at ^{119} Sn sites were detected as shown in Fig. 13 [96]. In the phase diagram of Cr–Sn, there is no magnetic phase besides pure Cr layers. The observation of magnetically split Sn spectra at room temperature proves that the thin Cr layers have a magnetic order with a fairly high transition temperature. The large hyperfine field means a significant penetration of spin polarization from Cr to Sn layers, and the spin arrangement at Cr interfaces should be ferromagnetic. However, it is not clarified yet what is the role of the own magnetic order of Cr in GMR properties.

4. Concluding remarks

Several Mössbauer spectroscopic studies on magnetic multilayers systems and of interface magnetism are described. It is demonstrated that ^{57}Fe is a useful probe to study magnetic properties in Fe layers, such as Fe/Cr interface roughness, metastable FCC-Fe/Cu(0 0 1) and chemically ordered FePt/MgO(0 0 1) films. Perpendicular Fe-spin orientation in rare-earth/Fe multilayers, and Mössbauer detection of perpendicular magnetic domains in Tb/Fe multilayers and their magnetization process in external fields are described. Evidence for closure domains in Co/Au multilayers is provided. For the study of non-magnetic layers, ^{197}Au and ^{119}Sn are useful Mössbauer probes. Although Au is popular as spacer layer material, ^{197}Au Mössbauer techniques have not yet been utilized sufficiently. The main reason is the inconvenience due to the short life-time of the γ-ray source. Because the γ-ray energy is relatively high, the measurements are limited to low temperatures. Since ^{197}Au is the only stable isotope, the position-selective enrichment technique cannot be applied,

i.e. Mössbauer spectra always show the situation of the total Au layer. To deduce information on the interface, it is necessary to compare spectra for different Au thicknesses. In the case of ^{119}Sn spectroscopy, Mössbauer measurements are technically very easy. Using samples with local enrichments in ^{119}Sn, position-selective information is available. However, the structure of the matrix layer is possibly disturbed by inserting ^{119}Sn probe layers, and a modification of the local electronic structure must be taken into consideration. It is certain that nuclear methods furnish us with unique information on magnetism in non-magnetic layers.

We did not discuss other important applications of ^{57}Fe Mössbauer spectroscopy, like thermal magnetic relaxation effects and spin-wave softening in magnetic films and superlattices. Here, we refer to the review by Walker [97]. Recently, magnetic relaxation effects and softening of the spin waves were observed in Fe/Ir(1 0 0) superlattices, which demonstrate the weak magnetic correlation from layer to layer in these magnetic heterostructures [98]. This is different from the behavior of epitaxial Fe(1 1 0)/Ag(1 1 1) superlattices with interlayer magnetic exchange coupling that oscillates as a function of the Ag interlayer thickness: these oscillations are reflected in a oscillatory slope of the hf field with temperature or oscillatory spin-wave stiffness parameter with Ag spacer thickness [99]. With the reduction of lateral dimensions of thin films and multilayers and the advent of magnetic nanowires and nanodots thermal spin fluctuations and superparamagnetism become increasingly important. Mössbauer spectroscopy is a suitable technique to study such phenomena on a time scale of $\sim 10^{-7}$ s [100–103]. Post-ion-implantation of ^{57}Co source atoms into nanodots might increase the detection sensitivity to the submonolayer range [104]. Furthermore, we anticipate exciting results from grazing incidence nuclear-resonant synchrotron Mössbauer reflectometry on ultrathin films and multilayers [105,106]. These experiments are performed in the time-differential mode. Nowadays, nuclear-resonant synchrotron experiments are feasible for ^{57}Fe, ^{119}Sn and ^{151}Eu isotopes. Recently, the Fe-spin orientation of epitaxial ultrathin (5 ML) anisotropic BCC-^{57}Fe islands on a stepped W(1 1 0) single-crystal surface in zero and non-zero external fields has been determined by nuclear-resonant synchrotron scattering with measurement times of only less than 30 min at the ESRF, Grenoble [107]. This may open the field for Mössbauer studies of large-area laterally-nanostructured magnetic systems. Thicker films (~ 1000 Å) can be investigated non-destructively along the film normal direction by depth-selective conversion electron Mössbauer spectroscopy (DCEMS) [108]. Moreover, inelastic nuclear-resonant absorption of synchrotron radiation may develop into an exciting technique for measuring vibrational density of states in magnetic multilayer systems [109].

Acknowledgements

The authors express their thanks to N. Hosoito, K. Kawaguchi, R. Yamamoto, Y. Endoh, N. Nakayama, T. Katamoto, K. Mibu, T. Emoto, S. Nasu, Y. Kobayashi, S. Tanaka, R.A. Brand, J. Jungermann, O. Marks, S. Neumann, T. Ruckert, J. Tappert, A. Schatz, B. Scholz, H. Schrör and particularly U. von Hörsten for their collaboration. Financial supports from Monbusho, NEDO, and the Deutsche Forschungsgemeinschaft (SFB166) are gratefully acknowledged.

References

[1] As an example of review: T. Shinjo, Surf. Sci. Rep. 12 (1991) 49.
[2] M.N. Baibich et al., Phys. Rev. Lett. 61 (1988) 2472.
[3] G. Binasch et al., Phys. Rev. B 39 (1989) 4828.
[4] M. Przybylski, Hyperfine Int. 113 (1998) 135.
[5] N. Hosoito, K. Kawaguchi, T. Shinjo, T. Takada, Y. Endoh, J. Phys. Soc. Japan. 53 (1984) 2659.
[6] N.K. Jaggi, L.H. Schwartz, J.K. Wong, J.B. Ketterson, J. Magn. Magn. Mater. 49 (1985) 1.
[7] K. Takanashi, H. Yasuoka, K. Kawaguchi, N. Hosoito, T. Shinjo, J. Phys. Soc. Japan 53 (1984) 4315.
[8] K. Kawaguchi, R. Yamamoto, N. Hosoito, T. Shinjo, T. Takada, J. Phys. Soc. Japan. 55 (1986) 211.
[9] N. Nakayama, T. Katamoto, T. Shinjo, J. Phys. F 18 (1989) 87.
[10] P.J. Schurer, Z. Celenski, B. Heinrich, Phys. Rev. B 48 (1993) 2577.
[11] P.J. Schurer, Z. Celenski, B. Heinrich, Phys. Rev. B 51 (1995) 2506.

[12] D.M. Kelly, E.E. Fullerton, P.T. Parker, J. Guimpel, Y. Bruynseraede, I.K. Schuller, Proceedings of the International Conference on Physics of Transition Metals, Darmstadt 1992, p. 419.
[13] R. Schad, P. Belien, G. Verbanck, K. Temst, V.V. Moshchalkov, Y. Bruynseraede, D. Bahr, J. Falta, J. Dekoster, G. Langouche, Europhys. Lett. 44 (1998) 379.
[14] J. Landes, Ch. Sauer, R.A. Brand, W. Zinn, S. Mantl, Zs. Kajcsos, J. Magn. Magn. Mater. 86 (1990) 71.
[15] F. Klinkhammer, Ch. Sauer, E. Yu Tsymbal, S. Handschuh, Q. Leng, W. Zinn, J. Magn. Magn. Mater. 161 (1996) 49.
[16] B. Drittler, N. Stefanou, S. Blügel, R. Zeller, P.H. Dederichs, Phys. Rev. B 40 (1989) 8203.
[17] Ch. Sauer, J. Landes, W. Zinn, H. Ebert, Mat. Res. Soc. Symp. Proc. 231 (1992) 153.
[18] J. Zukrowski, G. Liu, H. Fritzsche, U. Gradmann, J. Magn. Magn. Mater. 145 (1995) 57.
[19] D.L. Williamson, B.M. Lairson, A.P. Payne, N.M. Rensing, B.M. Clemens, Hyperfine Int. 92 (1994) 1271.
[20] N.M. Rensing, B.M. Clemens, D.L. Williamson, J. Appl. Phys. 79 (1996) 7757.
[21] B. Heinrich, J.F. Cochran, D. Venus, K. Totland, D. Atlan, S. Gorkov, K. Myrtle, J. Appl. Phys. 79 (1996) 4518.
[22] A. Davies, J.A. Stroscio, D.T. Pierce, R.J. Celotta, Phys. Rev. Lett. 76 (1996) 4175.
[23] For a review see: A.J. Freeman, R. Wu, J. Magn. Magn. Mater. 100 (1991) 497, and references therein.
[24] S. Ohnishi, A.J. Freeman, M. Weinert, Phys. Rev. B 30 (1984) 36.
[25] C.L. Fu, A.J. Freeman, J. Magn. Magn. Mater. 69 (1987) L1.
[26] K. Wagner, N. Weber, H.J. Elmers, U. Gradmann, J. Magn. Magn. Mater. 167 (1997) 21.
[27] J. Korecki, U. Gradmann, Europhys. Lett. 2 (1986) 651.
[28] M. Przybylski, J. Korecki, U. Gradmann, Appl. Phys. A 52 (1991) 33.
[29] S.C. Hong, A.J. Freeman, C.L. Fu, Phys. Rev. B 38 (1988) 12 156.
[30] U. Gradmann, J. Magn. Magn. Mater. 100 (1991) 481.
[31] Ch. Sauer, W. Zinn, in: L.H. Bennett, R.E. Watson (Eds.), Magnetic Multilayers, World Scientific, Singapore, 1993, references therein.
[32] Th. Detzel, N. Memmel, Th. Fauster, Surf. Sci. 293 (1993) 227.
[33] C.L. Fu, A.J. Freeman, Phys. Rev. B 35 (1987) 925.
[34] A. Schatz, Dissertation, Gerhard-Mercator-Universität Duisburg, Duisburg, Germany, 1996.
[35] D.J. Keavney, M.D. Wieczorek, D.F. Strom, J.C. Walker, J. Magn. Magn. Mater. 121 (1993) 49.
[36] G. Liu, U. Gradmann, J. Magn. Magn. Mater. 118 (1993) 99.
[37] W. Keune, A. Schatz, R.D. Ellerbrock, A. Fuest, Katrin Wilmers, R.A. Brand, J. Appl. Phys. 79 (1996) 4265, and references therein.
[38] M. Zharnikov, A. Dittschar, W. Kuch, C.M. Schneider, J. Kirschner, J. Magn. Magn. Mater. 174 (1997) 40, and references therein.
[39] Y. Yamada, B. Sadeh, C. Lee, M. Doi, M. Matsui, J. Magn. Soc. Japan 23 (1999) 575.
[40] V.L. Moruzzi, P.M. Marcus, J. Kübler, Phys. Rev. B 39 (1989) 6957.
[41] J. Shen, H. Jenniches, Ch.V. Mohan, J. Barthel, M. Klaua, P. Ohresser, J. Kirschner, Europhys. Lett. 43 (1998) 349.
[42] J. Shen et al., Phys. Rev. Lett. 80 (1998) 1980.
[43] Dongqi Li, D.J. Keavney, J. Pearson, S.D. Bader, J. Pege, W. Keune, Phys. Rev. B 57 (1998) 10 044.
[44] W.A.A. Macedo, F. Sirotti, G. Panaccione, A. Schatz, W. Keune, N.N. Rodrigues, R. Rossi, Phys. Rev. B 58 (1998) 11 534.
[45] W.A. Jesser, J.W. Matthews, Philos. Mag. 15 (1967) 1097.
[46] W.A. Jesser, J.W. Matthews, 17 (1968) 595.
[47] J. Thomassen, F. May, B. Feldmann, M. Wuttig, H. Ibach, Phys. Rev. Lett. 69 (1992) 3831.
[48] Dongqi Li, M. Freitag, J. Pearson, T.Q. Qiu, S.D. Bader, Phys. Rev. Lett. 72 (1994) 3112.
[49] S. Müller, P. Bayer, C. Reischl, K. Heinz, B. Feldmann, H. Zillgen, M. Wuttig, Phys. Rev. Lett. 74 (1995) 765.
[50] P. Bayer, S. Müller, P. Schmailzl, K. Heinz, Phys. Rev. B 48 (1993) 17611.
[51] W.A.A. Macedo, W. Keune, Phys. Rev. Lett. 61 (1988) 475.
[52] W. Keune, R. Halbauer, U. Gonser, J. Lauer, D.L. Williamson, J. Appl. Phys. 48 (1977) 2976.
[53] R. Halbauer, U. Gonser, J. Magn. Magn. Mater. 35 (1983) 55.
[54] W. Keune, T. Ezawa, W.A.A. Macedo, U. Glos, K.P. Schletz, U. Kirschbaum, Physica B 161 (1989) 269.
[55] D.J. Keavney, D.F. Storm, J.W. Freeland, I.L. Grigorov, J.C. Walker, Phys. Rev. Lett. 74 (1995) 4531.
[56] M. Maurer, J.C. Ousset, M. Piecuch, M.F. Ravet, J.P. Sanchez, Mat. Res. Soc. Symp. Proc. 151 (1989) 99.
[57] C.H. Herper, E. Hoffmann, P. Entel, Phys. Rev. B 60 (1999), in press.
[58] S. Blügel, H. Akai, R. Zeller, H. Dederichs, Phys. Rev. B 35 (1987) 3271.
[59] D. Guenzburger, D.E. Ellis, Phys. Rev. B 51 (1995) 12 519.
[60] E.F. Wassermann, J. Magn. Magn. Mater. 100 (1991) 346.
[61] R.J. Weiss, Proc. Phys. Soc. 82 (1963) 281.
[62] P. Entel, E. Hoffmann, P. Mohn, K. Schwarz, V.L. Moruzzi, Phys. Rev. B 47 (1993) 8706.
[63] M. Schröter, H. Ebert, H. Akai, P. Entel, E. Hoffmann, G.G. Reddy, Phys. Rev. B 52 (1995) 188.
[64] M.E. Gruner, R. Meyer, P. Entel, Europhys. J. B 2 (1998) 107.
[65] F.O. Schumann, S.Z. Wu, G.J. Mankey, R.F. Willis, Phys. Rev. B 56 (1997) 2668.
[66] J. Dresselhaus, M. Möller, Th. Kleemann, E. Kisker, J. Magn. Magn. Mater. 148 (1995) 172.
[67] J.W. Freeland, I.L. Grigorov, J.C. Walker, Phys. Rev. B 57 (1998) 80.

[68] U. Gradmann, H.O. Isbert, J. Magn. Magn. Mater. 15–18 (1980) 1109.
[69] S. Mitani, A. Kida, M. Matsui, J. Magn. Magn. Mater. 126 (1993) 76.
[70] K. Mibu, T. Shinjo, Hyperfine Int. 113 (1998) 287.
[71] For a review, see: Z.S. Shan, D.J. Sellmyer, in: K.A. Gschneider Jr., L. Eyring (Eds.), Handbook on the Physics and Chemistry of Rare Earths, Vol. 22, Elsevier, Amsterdam, 1996, p. 81, and references therein.
[72] K. Yoden, N. Hosoito, K. Kawaguchi, K. Mibu, T. Shinjo, Jpn. J. Appl. 27 (1988) 1680.
[73] B. Scholz, R.A. Brand, W. Keune, Phys. Rev. B 50 (1994) 2537, and references therein.
[74] J. Tappert, W. Keune, R.A. Brand, P. Vulliet, J.-P. Sanchez, T. Shinjo, J. Appl. Phys. 80 (1996) 4503.
[75] A. Hucht, K.D. Usadel, Phys. Rev. B 55 (1997) 12 309.
[76] Y. Millev, J. Kirschner, Phys. Rev. B 54 (1996) 4137.
[77] J. Teillet, F. Richomme, A. Fnidiki, M. Toulemonde, Phys. Rev. B 55 (1997) 11 560.
[78] J. Juraszek, A. Fnidiki, J. Teillet, F. Richomme, N.H. Duc, T.M. Dan, M. Toulemonde, W. Keune, Appl. Phys. Lett. 74 (1999) 2378.
[79] A. Gupta, A. Paul, R. Gupta, D.K. Avasthi, G. Principi, J. Phys.: Condens. Matter 10 (1998) 9669.
[80] J. Tappert, S. Neumann, R.A. Brand, W. Keune, F. Klose, and H. Maletta, Europhys. Lett. 46 (1999) 238.
[81] K. Cherifi, C. Dufour, M. Piecuch, A. Bruson, Ph. Bauer, G. Marchal, Ph. Mangin, J. Magn. Magn. Mater. 93 (1991) 609.
[82] F. Richomme, B. Scholz, R.A. Brand, W. Keune, J. Teillet, J. Magn. Magn. Mater. 156 (1996) 195.
[83] O. Marks, T. Ruckert, J. Tappert, W. Keune, W.-S. Kim, W. Kleemann, J. Voiron, IEEE Trans. Magn. 34 (1998) 834.
[84] N. Hamada, N. Hosoito, T. Shinjo, J. Phys. Soc. Japan 68 (1999) 1345.
[85] J.-U. Thiele, L. Folks, M.F. Toney, D.K. Weller, J. Appl. Phys. 84 (1998) 5686 and references therein.
[86] K. Takanashi, S. Mitani, M. Sano, H. Fujimori, H. Nakajima, A. Osawa, Appl. Phys. Lett. 67 (1995) 1016.
[87] A. Cebollada, D. Weller, J. Sticht, G.R. Harp, R.F.C. Farrow, R.F. Marks, R. Savoy, J.C. Scott, Phys. Rev. B 50 (1994) 3419.
[88] B.M. Lairson, M.R. Visokay, R. Sinclair, B.M. Clemens, Appl. Phys. Lett. 62 (1993) 639.
[89] M. Watanabe, M. Homma, Jpn. J. Appl. Phys. Part 2, 35 (1996) L1264.
[90] G.K. Wertheim, Mössbauer Effect: Principles and Applications, Academic, New York, 1964, p. 81.
[91] V. Gehanno, P. Auric, A. Party, B. Gilles, J. Magn. Magn. Mater. 188 (1998) 310.
[92] A. Fuss, S. Demokritov, P. Grünberg, W. Zinn, J. Magn. Magn. Mater. 103 (1992) L221.
[93] Y. Kobayashi, S. Nasu, T. Emoto, T. Shinjo, Hyperfine Int. 111 (1998) 129.
[94] T. Emoto, N. Hosoito, T. Shinjo, J. Magn. Magn. Mater. 189 (1998) 136.
[95] P. Sonntag, P. Bödeker, T. Thurston, H. Zabel, Phys. Rev. B 52 (1995) 7363.
[96] K. Mibu, S. Tanaka, T. Shinjo, J. Phys. Soc. Japan. 67 (1998) 2633.
[97] J.C. Walker, in: B. Heinrich, J.A.C. Bland (Eds.), Ultrathin Magnetic Structures II, Springer, Berlin, 1994, p. 327.
[98] Ph. Bauer, S. Andrieu, O.M. Lemine, M. Piecuch, J. Magn. Magn. Mater. 165 (1997) 220.
[99] D.J. Keavney, D.F. Strom, M.D. Wieczorek, J.C. Walker, J. Magn. Magn. Mater. 121 (1993) 283.
[100] S. Morup, J.A. Dumesic, D.H. Topsoe, in: R.L. Cohen (Ed.), Applications of Mössbauer Spectroscopy, vol. II, Academic, New York, 1980, pp. 1–53.
[101] D.G. Rancourt, S.R. Julian, J.M. Daniels, J. Magn, Magn. Mater. 49 (1985) 305; D.H, Jones, K.K.P. Srivastava, J. Magn. Magn. Mater. 78 (1989) 320.
[102] S. Linderoth, L. Balcells, A. Labarta, J. Tejada, P.V. Hendriksen, S.A. Sethi, J. Magn. Magn. Mater. 124 (1993) 269.
[103] H.-D. Pfannes, Hyperfine Int. 110 (1997) 127.
[104] J. Verheyden, S. Bukshpan, J. Dekoster, A. Vantomme, W. Deweerd, K. Milants, T. Barancira, G.L. Zhang, H. Pattyn, Europhys. Lett. 37 (1997) 25.
[105] T.S. Toellner, W. Sturhahn, R. Röhlsberger, E.E. Alp, C.H. Sowers, E.E. Fullerton, Phys. Rev. Lett. 74 (1995) 3475.
[106] L. Bottyan, J. Dekoster, L. Deak, A.Q.R. Baron, S. Degroote, R. Moons, D.L. Nagy, G. Langouche, Hyperfine Int. 113 (1998) 295.
[107] R. Röhlsberger, J. Bonsmann, private communication.
[108] S. Kruijer, O. Nikolov, W. Keune, H. Reuther, S. Weber, S. Scherrer, J. Appl. Phys. 84 (1998) 6570.
[109] W. Sturhahn, R. Röhlsberger, E.E. Alp, T. Ruckert, H. Schrör, W. Keune, J. Magn. Magn. Mater., in press.